

# Broad-Based Quantitative Structure–Activity Relationship Modeling of Potency and Selectivity of Farnesyltransferase Inhibitors Using a Bayesian Regularized Neural Network

Mitchell J. Polley,<sup>†</sup> David A. Winkler,<sup>\*,†,§</sup> and Frank R. Burden<sup>†,§,‡</sup>

Centre for Complexity in Drug Design, CSIRO Molecular Science, Private Bag 10, Clayton South MDC, Clayton 3169, Australia, Chemistry Department, Monash University, Clayton 3168, Australia, and SciMetrics, 23 Harrow Street, Blackburn South 3130, Australia

Received May 25, 2004

Inhibitors of the enzyme farnesyltransferase show potential as novel anticancer agents. There are many known inhibitors, but efforts to build predictive SAR models have been hampered by the structural diversity and flexibility of inhibitors. We have undertaken for the first time a QSAR study of the potency and selectivity of a large, diverse data set of farnesyltransferase inhibitors. We used novel molecular descriptors based on binned atomic properties and invariants of molecular matrices and a robust, nonlinear QSAR mapping paradigm, the Bayesian regularized neural network. We have built robust QSAR models of farnesyltransferase inhibition, geranylgeranyltransferase inhibition, and *in vivo* data. We have derived a novel selectivity index that allows us to model potency and selectivity simultaneously and have built robust QSAR models using this index that have the potential to discover new potent and selective inhibitors.

## Introduction

Farnesyl protein transferase (FT) is a heterodimeric zinc-catalyzed enzyme involved in the modulation of runaway cell replication in cancerous tumors.<sup>1–5</sup> FT is a member of the small family of protein prenylation enzymes that attach 15- or 20-carbon lipophilic chains to a number of cytosolic proteins.<sup>1,4,6</sup> This modification allows the prenylated protein to anchor to the inside surface of the cell membrane and usually results in the activation of a farnesylated protein so modified.<sup>1,3,5,7</sup>

Because of this, it was thought that direct inhibition of FT could be used to modulate the activity of mutated Ras proteins and thus attenuate runaway cell replication in cancerous tumors.<sup>1,3–4,6</sup> While inhibition of FT definitely shows promising results,<sup>4,5</sup> it is becoming apparent that this downstream effect may not be due entirely to the reduced numbers of farnesylated Ras oncoproteins but also possibly due to the reduced activity of other proteins that require farnesylation.<sup>1,3,4,6,7</sup> While the exact mechanism of action against the disease state remains unclear, FT inhibition does provide a promising avenue for antitumor therapeutic agents with fewer cytotoxic side effects than conventional chemotherapy.<sup>1,3</sup>

Three FTase inhibitors (FTIs) are currently in clinical trials with a fourth having been withdrawn for toxicity reasons.<sup>4</sup> The peptidomimetic substrate analogue L-778,123 is active in the sub-2.0 nM range with a 49-fold specificity for FT over another important protein prenylation enzyme, geranylgeranyltransferase (GGT).<sup>4,8</sup> The compound was withdrawn from clinical trials

because of unexpected cardiac effects.<sup>4</sup> The non-thiol-containing, benzodiazepine-like compound BMS-214662 was originally identified by screening assays.<sup>8</sup> It is active in the 1–10 nM range with a 1000-fold specificity for FT over GGT.<sup>4,8</sup> It displays good oral bioavailability and pharmacokinetic properties but during trials exhibited gastrointestinal toxicity, and the delivery method was changed to infusion only.<sup>4</sup> Initially identified as an antifungal compound,<sup>4</sup> R115777 is another FT inhibitor identified by screening.<sup>9</sup> It is a nonpeptidomimetic substituted quinolone that is active in 75% of cell lines investigated<sup>4</sup> and inhibits farnesylation of K-ras at 7.9 nM.<sup>8</sup> It is rapidly absorbed<sup>8</sup> and is well tolerated at pharmacologically relevant serum concentrations with some toxic effects observed.<sup>4</sup> The fused tricycle motif of the non-thiol-containing inhibitor SCH66336 inhibits in the range of 1–6 nM concentrations.<sup>4</sup> It has been shown to be active on a wide range of human tumor xenografts with favorable pharmacokinetics and absorption in animal models.<sup>4</sup> In clinical trials it shows inhibition at clinically relevant doses but suffers from some gastrointestinal effects.<sup>4</sup>

In terms of molecular modeling of FTIs, there is relatively little published in the area of predictive modeling and even less in the area of quantitative structure–activity relationship (QSAR). Most modeling studies are centered around corroborative modeling studies rather than predictive. While many studies imply that the results could have predicted the outcome of the synthetic efforts, they are never couched in explicit terms and thus can only be read as corroborative or supportive modeling.

The corroborative modeling studies on FTIs cover a wide range of techniques. Several previous studies have utilized X-ray analysis to elucidate structural aspects of the enzyme,<sup>10–12</sup> the inhibitors,<sup>13–18</sup> or both.<sup>19,20</sup> One

\* To whom correspondence should be addressed. Phone: +61-3-9545-2477. Fax: +61-3-9545-2446. E-mail: dave.winkler@csiro.au.

<sup>†</sup> CSIRO Molecular Science.

<sup>§</sup> Monash University.

<sup>‡</sup> SciMetrics.

study uses the enzyme structure of FT to illustrate an unusual catalytic mechanism,<sup>21</sup> while others identify residues and conformations important for substrate binding and catalysis.<sup>22,23</sup> Some of the simplest corroborative studies are those where the structure of a synthetic product is superimposed over that of a ligand cocrystallized with FT or an NMR ligand structure to illustrate a putative binding mode or active conformation.<sup>24–27</sup> More advanced and in-depth corroborative studies have mostly employed docking as a tool to provide insight into successful synthetic directions or to probe the receptor structure, along with other techniques.<sup>28–36</sup>

Several researchers have reported relatively narrow-focus predictive modeling studies of FTIs, usually centered on a pharmacophore hypothesis directing synthetic efforts.<sup>37,38</sup> Of slightly more significance are two more in-depth predictive modeling studies, one of which combines both predictive and corroborative docking,<sup>39</sup> the other of which uses predictive docking and reports inhibitors active in the 100 nM range.<sup>40</sup> There are a small number of modeling studies on FT that attempt limited predictive activity modeling. Of these, one in particular does not come under the heading of QSAR but does provide an extremely comprehensive and very well presented SAR model for a large congeneric series of fused tricycle inhibitors.<sup>41</sup> Another study utilizes a fusion of pharmacophore with QSAR studies, again derived from congeneric tricyclic inhibitors, to perform virtual screening on a database of compounds and rank them on the basis of predicted activity.<sup>42</sup> The predictive model used fitting to a pharmacophore as the descriptor for the SAR and proved to be quite adequate with the authors reporting that some compounds identified by this virtual screening method were active at 200 nM.<sup>42</sup> A second virtual screening study used predictive docking studies to estimate pseudo binding affinities as a score for selecting candidates from the Available Chemicals Directory for testing.<sup>43</sup> The study reported that of those selected for screening, active hits were found with  $IC_{50}$  of 25  $\mu$ M, but while the correlation between activity and estimated binding affinity seemed weak, screening of randomly selected compounds showed that the methods utilized were providing enrichment.<sup>43</sup>

Of more significance is an in depth study, using various modeling techniques as well as X-ray crystallography and wet chemistry, of the binding modes of congeneric tricyclic FTIs.<sup>44</sup> Possibly the most interesting result in the study, however, was the observation that for a small series of compounds the experimentally determined  $\Delta H^\circ$  of binding scaled linearly with the nonpolar surface area of the molecule that could be determined as “buried” in the X-ray crystal structures. This was quantified at 1 kcal/mol of  $\Delta H^\circ_{\text{bind}}$  for every 20  $\text{\AA}^2$  of buried nonpolar surface, which provides an important insight into the role of lipophilicity in FT inhibition.<sup>44</sup> When considering the chemical nature of the farnesyl moiety itself, it would appear in hindsight that this lipophilic importance is obvious; however, it is interesting to see it displayed so graphically in an inhibitor series and as such could be cause for thought when choosing descriptors for QSAR.

Only a few papers have reported broad-range QSAR studies on FTIs. One group used a system of multiple

techniques coupled with handpicked thermodynamic, physical, and topological descriptors to build a discriminatory model that could separate actives from inactives.<sup>45</sup> However, the compounds used for training were highly analogous, with activity apparently hinging on a few key structural features.<sup>45</sup> Another group used a diverse training set of anticancer compounds to compute a fragment-based QSAR model that could be subsequently employed to compute the probability of a particular compound being active against cancer.<sup>46</sup> The model was tested against a set of known FTIs and performed well, identifying the vast majority of them as inhibitors. The model was further tested by screening hypothetical inhibitors, which were subsequently synthesized and bioassayed.

There are a few examples of 2D and 3D QSAR analyses on FTIs,<sup>47–49</sup> and these are restricted to small data sets of congeneric series of analogues. Many of the 3D QSAR techniques, such as GRID,<sup>50</sup> CoMFA,<sup>51</sup> and CoMSIA<sup>52</sup> require molecules to be aligned prior to analysis. When considering the structural diversity of FTIs, it becomes obvious that performing such alignments would become problematic in this context; the structures are so diverse that deriving consistent alignment rules would be extremely difficult. It would even become a possibility that the alignment rules themselves could become the discriminating descriptor in the QSAR rather than those intended.

Traditional 2D QSAR methodologies do not need the alignment protocols that most 3D techniques require and usually benefit from an abundance of active compound data. However, with large data sets a dearth of structural diversity can lead to situations where models become harder to produce, less predictive, and less robust. This is usually caused by nonlinearity in the data response and descriptors with low information content. Adding more descriptors will sometimes alleviate this problem but will surely lead to an increased probability of chance correlation between the descriptors and the activity data.<sup>53,54</sup> Meanwhile, in areas such as FTIs, these problems are typically circumvented by avoiding QSAR studies on anything but series of molecular analogues. In this manner, only specialized descriptors are required to express the QSAR of the structurally similar series, leading to smaller numbers of descriptors that have a focused applicability to the problem at hand. This in turn leads to a lack of broad-based QSAR studies and focuses effort on compound series optimization while ignoring novel discovery through models that are not optimized for any particular molecular scaffold.

In this context, the aim of this paper is to show that by use of robust data-fitting methods and simple but information-rich descriptors it is possible to derive reliable broad QSAR models from sets of highly diverse molecules. This is accomplished by using a previously described Bayesian regularized artificial neural network (BRANN)<sup>55</sup> to generate a QSAR model on a large FTI data set, with subsequent comparison of this model to other models created using more traditional regression techniques.

## Materials and Methods

The data sets contained a diverse range of chemotypes: peptides, peptidomimetics, benzophenones, naphthalenes, mac-

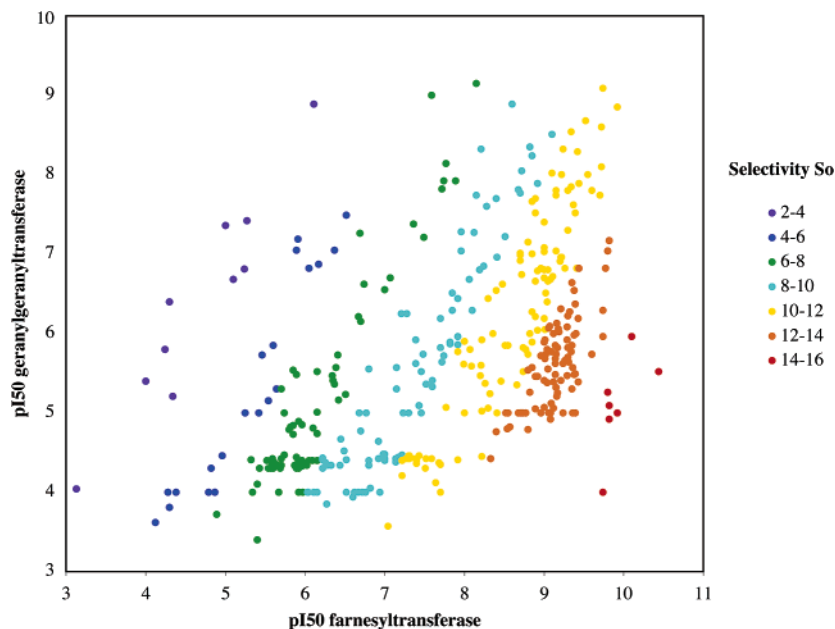


**Figure 1.** Plot of  $pK_i(\text{FT})$  vs  $pK_i(\text{GGT})$ . The points are color-coded for the optimal selectivity index  $S_o$ .

rocycles, chalcones, various mono-, di-, and tricyclic heterocycles, acrylamides, steroids, benzamides, benzodiazepines, and cinnamic acids.

**Farnesyltransferase Inhibitor (FTI) Data Set.** This set of 1687 compounds was compiled from available literature studies of FTIs.<sup>1,4,13-17,20,25-46,56-93</sup> Of those, only 1412 molecules were deemed fit for the analysis, with 275 being disqualified for a lack of, or uncertainty in, inhibition data versus the human isoform of the enzyme. The remaining molecules were split into two groups: a training set and a test set, with the test set comprising 20% (283) and the training set comprising 80% (1129) of the compounds. Test set compounds were selected on the basis of representative sampling of *k*-means clustering in descriptor space. This involved choosing one compound from each of 283 clusters for the test set, with the remainder forming the training set.

**Geranylgeranyltransferase Inhibitor (GGTI) Data Set.** This set of 446 compounds was compiled from available literature studies of FTIs.<sup>1,4,13-17,20,25-46,56-93</sup> These molecules were deemed fit for the analysis, having reliable inhibition data versus the human isoform of the enzyme. The molecules were split into two groups: a training set and a test set, with the test set comprising 20% (89) and the training set comprising 80% (357) of the compounds. Test set compounds were selected on the basis of representative sampling of *k*-means clustering in descriptor space.

**Tumor Cell Cytotoxicity (In Vivo) Data Set.** This set of compounds was compiled from available literature studies of FTIs.<sup>1,4,13-17,20,25-46,56-93</sup> The available in vivo data were whole-cell assays reported as the concentration required to inhibit either COS or NIH3T3 tumor cell-line proliferation by 50%. The number of molecules with in vivo data available was 232 for the NIH3T3 and 132 for the COS cell lines. Again, both of these data sets were partitioned into a training set consisting of 80% of the data set and into a test set comprising the remaining 20%. Both of these tumor lines are sensitive to FTIs.

**Selectivity Index.** Many papers have attempted to quantify the selectivity of bioactive compounds by computing the ratio of biological activity in one assay system to that in another. This is commonly done by the ratio of off-target  $K_i$  to target  $K_i$ . It can equally be computed as the ratio of toxic concentration to effective concentration (a therapeutic index) or as a similar ratio expressed for other free-energy-related biological endpoints such as the  $\text{IC}_{50}$  values used in this study. A significant problem with expressing selectivity this way is that it does not account for potency. Clearly the most desirable

outcome in drug research is to find compounds that simultaneously have high selectivity *and* high potency. A simple ratio of  $K_i$  or similar values does not discriminate between compounds that are, for example, 100-fold selective with potency of 1 mM or 1 nM. We have developed a simple expression that combines potency and selectivity, allowing both to be modeled and optimized simultaneously.

We define the optimal selectivity,  $S_o$ , by multiplying the simple selectivity defined above by a factor that weights the selectivity to favor selective and potent compounds. In the case of selectivity for FT over GGT in this work,

$$S_o = \left( \frac{1}{K_i^{\text{FT}}} \right) \left( \frac{K_i^{\text{GGT}}}{K_i^{\text{FT}}} \right) = \frac{K_i^{\text{GGT}}}{(K_i^{\text{FT}})^2}$$

The log of  $S_o$  is used to build QSAR models, where

$$\log S_o = 2 \text{p}K_i^{\text{FT}} - \text{p}K_i^{\text{GGT}}$$

or in terms of  $\text{IC}_{50}$  values,

$$\log S_o = 2 \text{p}I_{50}^{\text{FT}} - \text{p}I_{50}^{\text{GGT}}$$

The efficacy of this type of optimum selectivity index is illustrated in Figure 1, which shows the FT activity versus GGT activity, with compounds color-coded for optimum selectivity index. Clearly the highly potent, highly selective compounds are tightly clustered and are well represented by the  $S_o$  index. We used the FTI and GGTI data sets described above to form the optimum selectivity index and divided this data set into a training set (80%) and test set (20%), as with previous data sets.

**Molecular Descriptors.** QSAR studies may be divided into two types, depending on the purpose of the study. *Interpretive* studies generally aim to understand how the descriptors found to be important in a model relate to the interactions between the ligand and target. These studies often use a relatively small number of compounds whose biological properties have been carefully measured and molecular descriptors that can be easily related to structural characteristics. *Predictive* QSAR studies attempt to find QSAR models with the best predictive ability, usually using large, diverse data sets, sometimes less precise biological data, and computationally efficient descriptors. The study presented here is of the latter type: predictive modeling. Consequently, we employ molecular descriptors chosen for their computational efficiency and information-rich

**Table 1.** Quality of Models Derived from Farnesyltransferase Data Set Using Various Regression Methods

method	SEE	$R^2$	SEP	$Q^2$
MLR	0.137	0.743	0.149	0.700
PCR <sup>a</sup>	0.139	0.732	0.147	0.715
PLS <sup>b</sup>	0.139	0.736	0.147	0.710
BRANN <sup>c</sup>	0.100	0.860	0.126	0.76

<sup>a</sup> Using 34 principal components. <sup>b</sup> Using 11 components. <sup>c</sup> Using one three-neurode hidden layer.

character. The descriptors selected were the atomistic (*A*),<sup>94</sup> Burden (*B*),<sup>95</sup> and charge fingerprint (*C*) indices.<sup>96</sup> The *A* indices are simple counts of each type of atom in the molecule (which has been shown to correlate with lipophilicity and molecular refractivity),<sup>94</sup> and the *B* indices are widely known descriptors derived from the eigenvalues of modified adjacency matrices obtained from the connection table of the molecule. The charge fingerprint indices (*C*) are tallies of the number of atoms within a molecule, for which the calculated Gasteiger–Marsili charges<sup>97</sup> are binned into specified ranges. Essentially atom charges for each elemental type are binned into one of three bins. The  $3N$  bins (where  $N$  is the number of elemental atom types in the data set) are used as “fingerprint” descriptors. These encode electronic properties of the molecules in the data set and indirectly hydrophobic/hydrophilic properties. A more complete description of this method will be published shortly.<sup>96</sup>

**Regression Techniques.** The linear regression techniques used for this study were multiple linear regression (MLR), partial least squares (PLS), and principal components regression (PCR). Additionally, a previously published Bayesian regularized artificial neural network (BRANN)<sup>55</sup> was used to generate nonlinear QSAR models of the data. The architecture of the neural network used in this study comprised one hidden layer of three neurodes. We also carried out modeling with four neurodes to ensure that three are sufficient. The regression techniques were employed to correlate the molecular descriptors against the available *in vitro*  $-\log IC_{50}$  ( $pI_{50}$ ) data for the human isoform of FT, GGT, and the optimum selectivity index  $S_o$ . They were also used to build QSAR models of COS and of NIH3T3 cell *in vivo* toxicity.

**Software.** Descriptor and regression calculations were carried out using a purpose-developed software package called MolSAR, written in the Python programming language ([www.python.org](http://www.python.org)). MolSAR can rapidly calculate a range of molecular descriptors and perform several types of linear and nonlinear regression.

## Results and Discussion

The use of conventional linear regression methods combined with a selection of simple but information-dense molecular descriptors yielded QSAR models for FTIs, GGTIs, selectivity, and *in vivo* activities of reasonable quality (Table 1). However, the Bayesian neural network produced clearly superior models, as the following analyses show.

**FT Inhibition.** For the training set compounds the linear models all produced a standard error of estimation (SEE) of 13.7–13.9% and  $R^2$  in the range 0.73–0.74. The test set compounds gave a standard error of prediction (SEP) of 14.7–14.9% with  $Q^2$  ranging from 0.70 to 0.72. These models can all be considered to be of similar quality and of good predictive ability. This is to be expected because they are all fundamentally similar linear regression methods.

The models created using the Bayesian neural network exhibit distinctly higher statistical quality (Table 1 and Figure 2). By use of the BRANN, the training set SEE is reduced to 10% with an  $R^2$  of almost 0.86. The test set SEP is also substantially better at 12.6% with

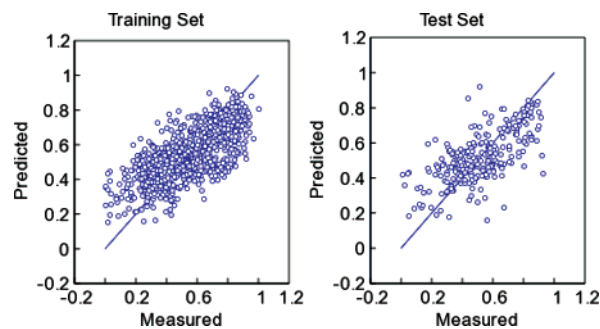


**Figure 2.** Bayesian regularized artificial neural network regression of FTI data set using one hidden layer with three neurodes. Data are scaled from 0 to 1.

a  $Q^2$  of 0.76. These improved statistics are reflected in the measured versus predicted plots for the QSAR model derived by the neural network (Figure 2), which generally shows a much tighter distribution of points than those for the linear models.

The improved models generated by the nonlinear neural network methods imply that the structure–activity relationship of the FTI data set has a nonlinear component. If such model-free nonlinear methods are employed to build a model, our work shows that complex and structurally diverse data sets can be well described by very simple molecular descriptors. The simple descriptors used in this study contain sufficient relevant information for even the linear regression methods to produce good models.

Comparison of our work with previous modeling studies of FTIs is difficult because there have been no broad-based QSAR studies performed. Published work tended to describe qualitative studies and hybrid SAR methods for virtual screening. Kaminski et al.<sup>42</sup> produced a QSAR model where the sole descriptor was a molecular fit to a pharmacophore hypothesis. This resulted in a model geared toward the discovery of compounds that would fit that hypothesis, and while it did indeed show some enrichment, there was no comparison of how well the predicted activities translated into experimental activities. The form of the model and descriptors, coupled to a lack of validation statistics, makes it impossible to perform a comparison. Similarly with Giraud et al.<sup>45</sup> and Estrada et al.,<sup>46</sup> the techniques and descriptors make a comparison difficult. The Giraud et al.<sup>45</sup> model is created on a highly congeneric series of molecules where one or two key structural differences correlate to activity and inactivity with descriptors that were not well described. Their PLS models reported a  $Q^2$  in the range 0.56–0.59, which is significantly smaller than the linear and nonlinear regression models derived from a much larger, diverse data set in our study. Estrada et al.<sup>46</sup> used their TOSS-MODE technique<sup>98</sup> to create a model that uses substructural fragments to calculate a probability of anticancer activity. Again, a direct comparison of the models or statistics is very difficult because the TOSS-MODE model is qualitative rather than quantitative. Three QSAR studies reported to date have involved small data sets and limited molecular diversity. Wan, Yi, and Guo carried out a CoMFA study<sup>47</sup> on 69 1-(8-chloro-6,11-dihydro-5*H*-benzo-[5,6]cyclohepta[1,2-*b*]pyridin-11-yl)piperazines. They obtained models with a cross-validated  $Q^2$  of 0.581, training set  $R^2$  of 0.968, and an SEE of 0.148. The

**Table 2.** Quality of Models Derived Using Bayesian Regularized Neural Networks with One Three-Neurode Hidden Layer and *ABC* Descriptors

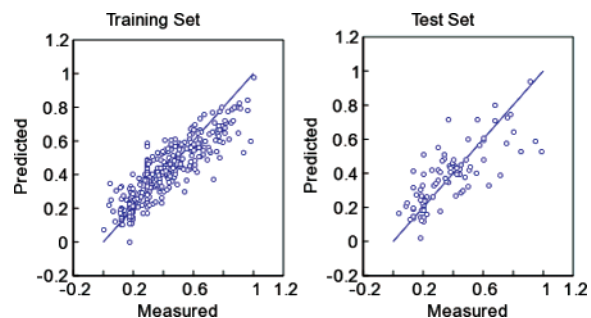
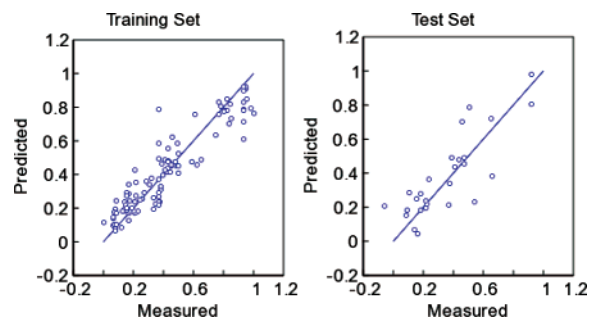
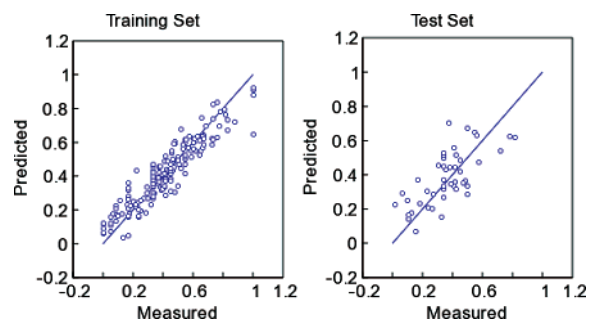
data set	SEE	$R^2$	SEP	$Q^2$	
FT	1412	0.100	0.860	0.126	0.760
GGT	446	0.093	0.893	0.138	0.778
COS cell	132	0.102	0.928	0.144	0.828
NIH3T3 cell	232	0.086	0.912	0.132	0.706
$S_o$	446	0.092	0.878	0.126	0.768

activities of 10 inhibitors predicted using this 3D QSAR model were in good agreement with the experimental activities. In an earlier paper,<sup>48</sup> these authors reported a CoMFA study of 32 2,3,4,5-tetrahydro-1-(1*H*-imidazol-4-ylmethyl)-4-(2-biphenylcarbonyl)-1*H*-1,4-benzodiazepine FTIs. The resulting model had a cross-validated  $Q^2$  of 0.602, training  $R^2$  of 0.958, and an SEE of 0.270. Sung and co-workers<sup>49</sup> reported a classical QSAR and Free-Wilson study of a small series of substituted heterocyclic chalcone derivatives. Their data set did not show a valid model, and they reported that the unsubstituted chalcone had the greatest FTI activity. Again, all three of these 2D and 3D QSAR studies had cross-validated statistics inferior to those reported here for test sets, despite the data sets being much smaller and much less diverse.

While the primary purpose of this study is to develop predictive QSAR models for virtual screening, it is possible to do some limited interpretation of the descriptors most relevant to the model. Among the most relevant descriptors were the numbers of  $sp^2$ -hybridized oxygens,  $sp^2$ -hybridized sulfurs, sulfate sulfur atoms, the numbers of five- and six-membered rings, 6 out of the 10 Burden indices, the occupancy of medium and high nitrogen charge bins, low and high oxygen charge bins, and the occupancy of low-charge sulfur atoms. Many of these descriptors come as no surprise. The Burden indices are topological and describe the molecular graph; many of the atomistic descriptors are of a type that describes either potential molecular hydrogen bond interactions ( $sp^2$ -hybridized oxygens) or charge interactions (e.g., sulfate atoms or charges). The models also show a dependence on hydrogen and carbon binned charge descriptors, which may reflect the importance of subtle hydrophobic effects in the binding site. The sulfate sulfur atom count and high charge bin phosphorus count may be consistent with those molecules mimicking the diphosphate group of the farnesyl diphosphate cofactor, while the  $sp^2$ -hybridized sulfur count and low-charge sulfur count could be indicative of compounds possessing moieties that bind to the catalytic zinc ion.

The increase in  $R^2$  and  $Q^2$  of the BRANN models when compared to the linear models highlights the capacity for such technologies to provide better data-modeling capabilities for QSAR. This appears particularly true for systems such as farnesyltransferase where a large number of active compounds are available with a high degree of structural diversity.

**GGT Inhibition.** The statistical quality of the models produced with the GGTI data is shown in Table 2 and Figure 3. Limited analysis of this data set using linear methods compared with BRANNs showed a trend similar to that observed in the FTI data set. It is clear that the BRANN model has high statistical significance

**Figure 3.** Bayesian regularized artificial neural network regression of GGTI data set using one hidden layer with three neurodes. Data are scaled from 0 to 1.**Figure 4.** Bayesian regularized artificial neural network regression of COS cell in vivo data set using one hidden layer with three neurodes. Data are scaled from 0 to 1.**Figure 5.** Bayesian regularized artificial neural network regression of NIH3T3 cell in vivo data set using one hidden layer with three neurodes. Data are scaled from 0 to 1.

and has a very good predictive capability, as the statistics for the test set illustrate. The model had a training set SEP of 9.3% and  $R^2$  of 0.893, explaining almost 90% of the variance in the training set data. The test set was well predicted with an SEE of 13.8% and  $Q^2$  of 0.778.

**In Vivo Models.** The results of modeling the in vivo data for the COS and NIH3T3 tumor cell-line proliferation whole-cell assays are reported in Table 2 and Figure 4 (COS cells) and Figure 5 (NIH3T3 cells). It is clear that the models are also highly significant. The COS cell toxicity model had a training set SEE of 10.2% and  $R^2$  of 0.928. The test set statistics were also very good with SEP of 14.4% and  $Q^2$  of 0.828. The statistics for the NIH cell toxicity model were similar except for slightly lower values for the test set (SEP 13.2% and  $Q^2$  of 0.706).

**Selectivity Index.** The optimal selectivity index produced good models with the *ABC* descriptors as Figure 6 and Tables 2 and 3 illustrate. The model had excellent statistical significance, with a training set SEE of 9.2% and  $R^2$  of almost 0.88. The test set was also very

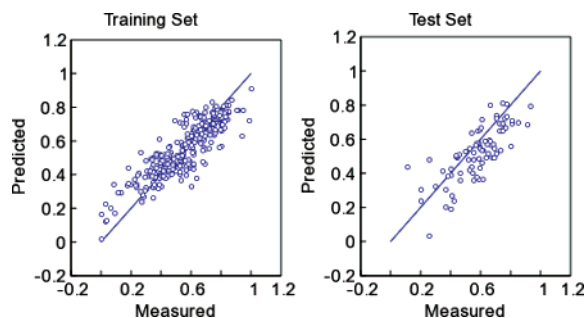


**Figure 6.** Bayesian regularized artificial neural network regression of optimal selectivity index  $S_0$  using one hidden layer with three neurodes. Data are scaled from 0 to 1.

**Table 3.** Descriptors Used for Deriving QSAR Models

index	name	descriptor
1	MolWt	molecular mass in daltons
2	A_0	hydrogen atom count
3	A_5	sp carbon atom count
4	A_6	sp <sup>2</sup> carbon atom count
5	A_7	sp <sup>3</sup> carbon atom count
6	A_8	aromatic carbon atom count
7	A_9	sp nitrogen atom count
8	A_10	sp <sup>2</sup> nitrogen atom count
9	A_11	sp <sup>3</sup> nitrogen atom count
10	A_13	aromatic nitrogen atom count
11	A_14	sp <sup>2</sup> oxygen atom count
12	A_15	sp <sup>3</sup> oxygen atom count
13	A_16	aromatic oxygen atom count
14	A_17	fluorine atom count
15	A_27	phosphate phosphorus atom count
16	A_30	sp <sup>2</sup> sulfur atom count
17	A_31	sp <sup>3</sup> sulfur atom count
18	A_33	sulfate sulfur atom count
19	A_35	chlorine atom count
20	A_53	bromine atom count
21	A_71	iodine atom count
22	G_3	count of atoms in three-membered rings
23	G_4	count of atoms in four-membered rings
24	G_5	count of atoms in five-membered rings
25	G_6	count of atoms in six-membered rings
26	G_7	count of atoms in seven-membered rings
27–36	E_0 to E_9	Burden indices (five lowest and five highest eigenvalues of the modified adjacency matrix)
37	BCGM_1	hydrogen partial charges, low bin
38	BCGM_2	hydrogen partial charges, mid bin
39	BCGM_3	hydrogen partial charges, high bin
40	BCGM_4	carbon partial charges, low bin
41	BCGM_5	carbon partial charges, low bin
42	BCGM_6	carbon partial charges, low bin
43	BCGM_7	nitrogen partial charges, low bin
44	BCGM_8	nitrogen partial charges, mid bin
45	BCGM_9	nitrogen partial charges, high bin
46	BCGM_10	oxygen partial charges, low bin
47	BCGM_11	oxygen partial charges, mid bin
48	BCGM_12	oxygen partial charges, high bin
49	BCGM_18	phosphorus partial charges, high bin
50	BCGM_19	sulfur partial charges, low bin
51	BCGM_20	sulfur partial charges, mid bin

well predicted with SEP of 12.6% and  $Q^2$  approaching 0.77. This clearly provides us with an excellent model for searching for potent and selective compounds in databases or virtual libraries.

## Conclusions

This work represents the first QSAR modeling study of farnesyltransferase and geranylgeranyltransferase inhibitors on such a large, diverse data set. The traditional linear regression methods created statistically

significant models, while the nonlinear methods created models with substantially higher significance. As with the models from previous studies, this work has generated a system capable of rapid virtual screening of compounds for FTI and anticancer activity. Unlike previous studies this model is derived from a set of known inhibitors that is structurally diverse and as a result should provide more robust extrapolation in chemistry space compared to models created on congeneric analogue series. In future development, this type of model could be highly advantageous because discovery efforts could take whole-cell activity into account, a point where many lead candidates often fall short because of poor cell-membrane partitioning.

**Acknowledgment.** The authors thank Tripos Inc. for contributing the majority of the farnesyltransferase database. The data set is available from the authors or from Tripos Inc. on request.

## References

- Leonard, D. M. Ras Farnesyltransferase: A New Therapeutic Target. *J. Med. Chem.* **1997**, *40*, 2971–2990.
- Park, H.-W.; Boduluri, S. R.; Moomaw, J. F.; Casey, P. J.; Beese, L. S. Crystal Structure of Protein Farnesyltransferase at 2.25 Angstrom Resolution. *Science* **1997**, *275*, 1800–1804.
- Cox, A. C.; Der, C. J. Farnesyltransferase inhibitors: promises and realities. *Curr. Opin. Pharmacol.* **2002**, *2*, 388–393.
- Haluska, P.; Dy, G. K.; Adjei, A. A. Farnesyl transferase inhibitors as anticancer agents. *Eur. J. Cancer* **2002**, *38*, 1685–1700.
- Ollif, A. Farnesyltransferase inhibitors: targeting the molecular basis of cancer. *Biochim. Biophys. Acta* **1999**, *1423*, C19–C30.
- Prendergast, G. C.; Oliff, A. Farnesyltransferase inhibitors: antineoplastic properties, mechanisms of action, and clinical prospects. *Semin. Cancer Biol.* **2000**, *10*, 443–452.
- Gibbs, J. B.; Graham, S. L.; Hartman, G. D.; Koblan, K. S.; Kohl, N. E.; Omer, C. A.; Oliff, A. Farnesyltransferase inhibitors versus Ras inhibitors. *Curr. Opin. Chem. Biol.* **1997**, *1*, 197–203.
- Sausville, E. A.; Elsayed, Y.; Monga, M.; Kim, G. Signal Transduction-Directed Cancer Treatments. *Annu. Rev. Pharmacol. Toxicol.* **2003**, *43*, 199–213.
- Johnston, S. R. D. Farnesyl transferase inhibitors: a novel targeted therapy for cancer. *Lancet Oncol.*, **2001**, *2*, 18–26.
- Long, S. B.; Casey, P. J.; Beese, L. S. Reaction path of protein farnesyltransferase at atomic resolution. *Nature* **2002**, *419*, 645–650.
- Park, H.-W.; Beese, L. S. Protein Farnesyltransferase. *Curr. Opin. Struct. Biol.* **1997**, *7*, 873–880.
- Tobin, D. A.; Pickett, J. S.; Hartman, H. L.; Fierke, C. A.; Penner-Hahn, J. E. Structural Characterization of the Zinc Site in Protein Farnesyltransferase. *J. Am. Chem. Soc.* **2003**, *125*, 9962–9969.
- Rawson, T. E.; Somers, T. C.; Marsters, J. C., Jr.; Wan, D. T.; Reynolds, M. E.; Burdick, D. J. Stereochemistry of the Benzodiazepine-Based Ras Farnesyltransferase Inhibitors. *Bioorg. Med. Chem. Lett.* **1995**, *5*, 1335–1338.
- Ohkanda, J.; Lockman, J. W.; Kothare, M. A.; Qian, Y.; Blaskovich, M. A.; Sebt, S. M.; Hamilton, A. D. Design and Synthesis of Potent Nonpeptidic Farnesyltransferase Inhibitors Based on a Terphenyl Scaffold. *J. Med. Chem.* **2002**, *45*, 177–188.
- Gwaltney, S. L., II; O'Connor, S. J.; Nelson, L. T. J.; Sullivan, G. M.; Imade, H.; Wang, W.; Hasvold, L.; Li, Q.; Cohen, J.; Gu, W.-Z.; Tahir, S. K.; Bauch, J.; Marsh, K.; Ng, S.-C.; Frost, D. J.; Zhang, H.; Muchmore, S.; Jakob, C. G.; Stroll, V.; Hutchins, C.; Rosenberg, S. H.; Sham, H. L. Aryl Tetrahydropyridine Inhibitors of Farnesyltransferase: Glycine, Phenylalanine and Histidine Derivatives. *Bioorg. Med. Chem. Lett.* **2003**, *13*, 1359–1362.
- Gwaltney, S. L., II; O'Connor, S. J.; Nelson, L. T. J.; Sullivan, G. M.; Imade, H.; Wang, W.; Hasvold, L.; Li, Q.; Cohen, J.; Gu, W.-Z.; Tahir, S. K.; Bauch, J.; Marsh, K.; Ng, S.-C.; Frost, D. J.; Zhang, H.; Muchmore, S.; Jakob, C. G.; Stroll, V.; Hutchins, C.; Rosenberg, S. H.; Sham, H. L. Aryl Tetrahydropyridine Inhibitors of Farnesyltransferase: Bioavailable Analogues with Improved Cellular Potency. *Bioorg. Med. Chem. Lett.* **2003**, *13*, 1363–1366.
- Curtin, M. L.; Florjancic, A. S.; Cohen, J.; Gu, W.-Z.; Frost, D. J.; Muchmore, S. W.; Sham, H. L. Novel and Selective Imidazole-Containing Biphenyl Inhibitors of Protein Farnesyltransferase. *Bioorg. Med. Chem. Lett.* **2003**, *13*, 1367–1371.
- Roskoski, R., Jr. Protein prenylation: a pivotal posttranslational process. *Biochem. Biophys. Res. Commun.* **2003**, *303*, 1–7.

- (19) Long, S. B.; Casey, P. J.; Beese, L. S. The basis for K-Ras4B binding specificity to protein farnesyltransferase revealed by 2 Å resolution ternary complex structures. *Structure* **2000**, *8*, 209–222.
- (20) deSolms, S. J.; Ciccarone, T. M.; MacTough, S. C.; Shaw, A. W.; Buser, C. A.; Ellis-Hutchings, M.; Fernandes, C.; Hamilton, K. A.; Huber, H. E.; Kohl, N. E.; Lobell, R. B.; Robinson, R. G.; Tsou, N. N.; Walsh, E. S.; Graham, S. L.; Beese, L. S.; Taylor, J. S. Dual Protein Farnesyltransferase-Geranylgeranyltransferase-I Inhibitors as Potent Cancer Chemotherapeutic Agents. *J. Med. Chem.* **2003**, *46*, 2973–2984.
- (21) Hightower, K. E.; Fierke, C. A. Zinc-catalysed sulphur alkylation: insights from protein farnesyltransferase. *Curr. Opin. Chem. Biol.* **1999**, *3*, 176–181.
- (22) Hightower, K. E.; De, S.; Weinbaum, C.; Spence, R. A.; Casey, P. J. Lysine164A of protein farnesyltransferase is important for both CaaX substrate binding and catalysis. *Biochem. J.* **2001**, *360*, 625–631.
- (23) Pickett, J. S.; Bowers, K. E.; Hartman, H. L.; Fu, H.-W.; Embry, A. C.; Casey, P. J.; Fierke, C. A. Kinetic Studies of Protein Farnesyltransferase Mutants Establish Active Substrate Conformation. *Biochemistry* **2003**, *42*, 9741–9748.
- (24) Williams, T. M.; Bergman, J. M.; Brashear, K.; Breslin, M. J.; Dinsmore, C. J.; Hutchinso, J. H.; MacTough, S. C.; Wei, D. D.; Zartman, C. B.; Bogusky, M. J.; Culbertson, J. C.; Buser-Doepner, C.; Davide, J.; Greenberg, I. B.; Hamilton, K. A.; Koblan, K. S.; Kohl, N. E.; Liu, D.; Lobell, R. B.; Mosser, S. D.; O'Neill, T. J.; Rands, E.; Schaber, M. D.; Wilson, F.; Senderak, E.; Motzel, S. L.; Gibbs, J. B.; Graham, S. L.; Heimbros, D. C.; Hartman, G. D.; Oliff, A. I.; Huff, J. R. *N*-Arylpiperazine Inhibitors of Farnesyltransferase: Discovery and Biological Activity. *J. Med. Chem.* **1999**, *42*, 3779–3784.
- (25) Dinsmore, C. J.; Bogusky, M. J.; Culbertson, J. C.; Bergman, J. M.; Homnick, C. F.; Zartman, C. B.; Mosser, S. D.; Schaber, M. D.; Robinson, R. G.; Koblan, K. S.; Huber, H. E.; Graham, S. L.; Hartman, G. D.; Huff, J. R.; Williams, T. M. Conformational Restriction of Flexible Ligands Guided by the Transferred NOE Experiment: Potent Macrocyclic Inhibitors of Farnesyltransferase. *J. Am. Chem. Soc.* **2001**, *123*, 2107–2108.
- (26) Schlitzer, M.; Böhm, M.; Sattler, I. Non-Thiol Farnesyltransferase Inhibitors: Structure–Activity Relationships of Benzophenone-Based Bisubstrate Analogue Farnesyltransferase Inhibitors. *Bioorg. Med. Chem.* **2002**, *10*, 615–620.
- (27) Ciccarone, T. M.; MacTough, S. C.; Williams, T. M.; Dinsmore, C. J.; O'Neill, T. J.; Shah, D.; Culbertson, J. C.; Koblan, K. S.; Kohl, N. E.; Gibbs, J. B.; Oliff, A. I.; Graham, S. L.; Hartman, G. D. Non-Thiol 3-Aminomethylbenzamide Inhibitors of Farnesyl-Protein Transferase. *Bioorg. Med. Chem. Lett.* **1999**, *9*, 1991–1996.
- (28) Schlitzer, M.; Böhm, M.; Sattler, I. Non-Peptidic, Non-Prenylic Bisubstrate Farnesyltransferase Inhibitors. Part 3: Structural Requirements of the Central Moiety for Farnesyltransferase Inhibitory Activity. *Bioorg. Med. Chem.* **2000**, *8*, 2399–2406.
- (29) Sakowski, J.; Böhm, M.; Sattler, I.; Dahse, H.-M.; Schlitzer, M. Synthesis, Molecular Modeling, and Structure–Activity Relationship of Benzophenone-Based CAAX-Peptidomimetic Farnesyltransferase Inhibitors. *J. Med. Chem.* **2001**, *44*, 2886–2889.
- (30) Böhm, M.; Mitsch, A.; Wissner, P.; Sattler, I.; Schlitzer, M. Exploration of Novel Aryl Binding Sites of Farnesyltransferase Using Molecular Modeling and Benzophenone-Based Farnesyltransferase Inhibitors. *J. Med. Chem.* **2001**, *44*, 3117–3124.
- (31) Sakowski, J.; Böhm, M.; Sattler, I.; Schlitzer, M. Non-Thiol Farnesyltransferase Inhibitors: Evaluation of Different AA(X)-Peptidomimetic Substructures in Combination with Arylic Cysteine Replacements. *Arch. Pharm. (Weinheim, Ger.)* **2002**, *4*, 135–142.
- (32) Pedretti, A.; Villa, L.; Vistoli, G. Modeling of Binding Modes and Inhibition Mechanism of Some Natural Ligands of Farnesyl Transferase Using Molecular Docking. *J. Med. Chem.* **2002**, *45*, 1460–1465.
- (33) Houssin, R.; Pommery, J.; Salaün, M.-C.; Deweer, S.; Goossens, J.-F.; Chavette, P.; Hénichart, J.-P. Design, Synthesis, and Pharmacological Evaluation of New Farnesyl Protein Transferase Inhibitors. *J. Med. Chem.* **2002**, *45*, 533–536.
- (34) Kettler, K.; Sakowski, J.; Silber, K.; Sattler, I.; Klebe, G.; Schlitzer, M. Non-thiol Farnesyltransferase Inhibitors: *N*-(4-Acylamino-3-benzoylphenyl)-3-[5-(4-nitrophenyl)-2-furyl]acrylic Acid Amides. *Bioorg. Med. Chem.* **2003**, *11*, 1521–1530.
- (35) Thutewohl, M.; Kissau, L.; Popkirova, B.; Karaguni, I.-M.; Nowak, T.; Bate, M.; Kuhlmann, J.; Müller, O.; Waldmann, H. Identification of Mono- and Bisubstrate Inhibitors of Protein Farnesyltransferase and Inducers of Apoptosis from a Peptidomimetic Library. *Bioorg. Med. Chem.* **2003**, *11*, 2617–2626.
- (36) Lannuzel, M.; Lamothe, M.; Schambel, P.; Etiévant, C.; Hill, B.; Perez, M. From Pure FPP to Mixed FPP and CAAX Competitive Inhibitors of Farnesyl Protein Transferase. *Bioorg. Med. Chem. Lett.* **2003**, *13*, 1459–1462.
- (37) Burns, C. J.; Guitton, J.-D.; Baudoin, B.; Lelièvre, Y.; Duchesne, M.; Parker, F.; Fromage, N.; Commeçon, A. Novel Conformationally Extended Naphthalene-Based Inhibitors of Farnesyltransferase. *J. Med. Chem.* **1997**, *40*, 1763–1767.
- (38) Hunt, J. T.; Ding, C. Z.; Batorsky, R.; Bednarz, M.; Bhide, R.; Cho, Y.; Chong, S.; Chao, S.; Gullo-Brown, J.; Guo, P.; Kim, S. H.; Lee, F. Y. F.; Leftheris, K.; Miller, A.; Mitt, T.; Patel, M.; Penhallow, B. A.; Ricca, C.; Rose, W. C.; Schmidt, R.; Slusarchyk, W. A.; Vite, G.; Manne, V. Discovery of (*R*)-7-Cyano-2,3,4,5-tetrahydro-1-(1*H*-imidazol-4-ylmethyl)-3-(phenylmethyl)-4-(2-thienylsulfonyl)-1*H*-1,4-benzodiazepine (BMS-214662), a Farnesyltransferase Inhibitor with Potent Preclinical Antitumor Activity. *J. Med. Chem.* **2000**, *43*, 3587–3595.
- (39) Xu, K.; Perola, E.; Prendergast, F. G.; Pang, Y.-P. Models of Ternary Complexes for Nonpeptidic Farnesyltransferase Inhibitors: Insights into Structure-Based Screen and Design of Potential Anticancer Therapeutics. *J. Mol. Model.* **1999**, *5*, 203–217.
- (40) Mitsch, A.; Böhm, M.; Wissner, P.; Sattler, I.; Schlitzer, M. Non-Thiol Farnesyltransferase Inhibitors: Utilization of an Aryl Binding Site by 5-Arylacryloylaminobenzophenones. *Bioorg. Med. Chem.* **2002**, *10*, 2657–2662.
- (41) Mallams, A. K.; Rossman, R. R.; Doll, R. J.; Girijavallabhan, V. M.; Ganguly, A. K.; Petrin, J.; Wang, L.; Patton, R.; Bishop, W. R.; Carr, D. M.; Kirschmeier, P.; Catino, J. J.; Bryant, M. S.; Chen, K.-J.; Korfmacher, W. A.; Nardo, C.; Wang, S.; Nomeir, A. A.; Lin, C.-C.; Li, Z.; Chen, J.; Lee, S.; Dell, J.; Lipari, P.; Malkowski, M.; Yaremko, B.; King, I.; Liu, M. Inhibitors of Farnesyl Protein Transferase. 4-Amido, 4-Carbamoyl, and 4-Carboxamido Derivatives of 1-(8-Chloro-6,11-dihydro-5*H*-benzo[5,6]-cyclohepta[1,2-*b*]pyridine-11-yl)piperazine and 1-(3-Bromo-8-chloro-6,11-dihydro-5*H*-benzo[5,6]-cyclohepta[1,2-*b*]pyridine-11-yl)piperazine. *J. Med. Chem.* **1998**, *41*, 877–893.
- (42) Kaminski, J. J.; Rane, D. F.; Snow, M. E.; Weber, L.; Rothofsky, M. L.; Anderson, S. D.; Lin, S. L. Identification of Novel Farnesyl Protein Transferase Inhibitors Using Three-Dimensional Database Searching Methods. *J. Med. Chem.* **1997**, *40*, 4103–4112.
- (43) Perola, E.; Xu, K.; Kollmeyer, Thomas, M.; Kaufmann, S. H.; Prendergast, F. G.; Pang, Y.-P. Successful Virtual Screening of a Chemical Database for Farnesyltransferase Inhibitor Leads. *J. Med. Chem.* **2000**, *43*, 401–408.
- (44) Strickland, C. L.; Weber, P. C.; Windsor, W. T.; Wu, Z.; Le, H. V.; Albanese, M. M.; Alvarez, C. S.; Cesarz, D.; del Rosario, J.; Deskus, J.; Mallams, A. K.; Njorge, F. G.; Piwinski, J. J.; Remiszewski, S.; Rossman, R. R.; Taveras, A. G.; Vibulbhan, B.; Doll, R. J.; Girijavallabhan, V. M.; Ganguly, A. K. Tricyclic Farnesyl Protein Transferase Inhibitors: Crystallographic and Calorimetric Studies of Structure–Activity Relationships. *J. Med. Chem.* **1999**, *42*, 2125–2135.
- (45) Giraud, E.; Luttman, C.; Lavelle, F.; Riou, J.-F.; Maillet, P.; Laoui, A. Multivariate Data Analysis Using D-Optimal Designs, Partial Least Squares, and Response Surface Modeling: A Directional Approach for the Analysis of Farnesyltransferase Inhibitors. *J. Med. Chem.* **2000**, *43*, 1807–1816.
- (46) Estrada, E.; Uriarte, E.; Montero, A.; Teijeira, M.; Santana, L.; De Clercq, E. A Novel Approach for the Virtual Screening and Rational Design of Anticancer Compounds. *J. Med. Chem.* **2000**, *43*, 1975–1985.
- (47) Wan, S.; Yi, X.; Guo, Z. Three-Dimensional Quantitative Structure–Activity Relationship of a Series of Benzo[cyclohepta]pyridine Farnesyltransferase Inhibitors. *Yaoxue Xuebao* **2002**, *37*, 257–262.
- (48) Wan, S.; Yi, X.; Guo, Z. Three-Dimensional Quantitative Structure–Activity Relationship of Farnesyl Protein Transferase Inhibitors. *Yaoxue Xuebao* **2001**, *36*, 423–426.
- (49) Sung, N.-D.; Yu, S.-J.; Myung, P.-K.; Kwon, B.-M. Quantitative Structure–Activity Relationship (QSAR) Analyses on the Farnesyl Protein Transferase Inhibition Activity of Hetero Ring Substituted Chalcone Derivatives by the Hansch and Free-Wilson Method. *Han'guk Nonghwa Hakhoechi* **2000**, *43*, 95–99.
- (50) Goodford, P. J. A Computational Procedure for Determining Energetically Favourable Binding Sites on Biologically Important Molecules. *J. Med. Chem.* **1985**, *28*, 849–857.
- (51) Cramer, R. D., III; Patterson, D. E.; Bunce, J. D. Comparative Molecular Field Analysis (CoMFA). 1. Effect of Shape on Binding of Steroids to Carrier Proteins. *J. Am. Chem. Soc.* **1988**, *110*, 5959–5967.
- (52) Klebe, G.; Abraham, U.; Mietzner, T. Molecular Similarity Indices in a Comparative Analysis (CoMSIA) of Drug Molecules To Correlate and Predict Their Biological Activity. *J. Med. Chem.* **1994**, *37*, 4130–4146.
- (53) Topliss, J. G.; Costello, R. J. Chance Correlations in Structure–Activity Studies Using Multiple Regression Analysis. *J. Med. Chem.* **1972**, *15*, 1066–1068.
- (54) Topliss, J. G.; Edwards, R. P. Chance Factors in Studies of Quantitative Structure–Activity Relationships. *J. Med. Chem.* **1979**, *22*, 1238–1244.

- (55) Burden, F. R.; Winkler, D. A. Robust QSAR Models Using Bayesian Regularized Neural Networks. *J. Med. Chem.* **1999**, *42*, 3183–3187.
- (56) Brown, M. S.; Goldstein, J. L.; Paris, K. J.; Burnier, J. P.; Marsters, J. C., Jr. Tetrapeptide inhibitors of protein farnesyltransferase: Amino-terminal substitution in phenylalanine-containing tetrapeptides restores farnesylation. *Proc. Natl. Acad. Sci. U.S.A.* **1992**, *89*, 8313–8316.
- (57) Gibbs, J. B.; Pompliano, D. L.; Mosser, S. D.; Rands, E.; Lingham, R. B.; Singh, S. B.; Scolnick, E. M.; Kohl, N. E.; Oliff, A. Selective Inhibition of Farnesyl-Protein Transferase Blocks Ras Processing in Vivo. *J. Biol. Chem.* **1993**, *268*, 7617–7620.
- (58) Hara, M.; Akasaka, K.; Akinaga, S.; Okabe, M.; Nakano, H.; Gomez, R.; Wood, D.; Uh, M.; Tamanoi, F. Identification of Ras Farnesyltransferase Inhibitors by Microbial Screening. *Proc. Natl. Acad. Sci. U.S.A.* **1993**, *90*, 2281–2285.
- (59) Graham, S. L.; deSolms, S. J.; Giuliani, E. A.; Kohl, N. E.; Mosser, S. D.; Oliff, A. I.; Pompliano, D. L.; Rands, E.; Breslin, M. J.; Deana, A. A.; Garsky, V. M.; Scholz, T. H.; Gibbs, J. B.; Smith, R. L. Pseudopeptide Inhibitors of Ras Farnesyl-Protein Transferase. *J. Med. Chem.* **1994**, *37*, 725–732.
- (60) Kohl, N. E.; Wilson, F. R.; Mosser, S. D.; Giuliani, E.; deSolms, S. J.; Conner, M. W.; Anthony, N. J.; Holtz, W. J.; Gomez, R. P.; Lee, T.-J.; Smith, R. L.; Graham, S. L.; Hartman, G. D.; Gibbs, J. B.; Oliff, A. Protein Farnesyltransferase Inhibitors Block the Growth of Ras-Dependent Tumors in Nude Mice. *Proc. Natl. Acad. Sci. U.S.A.* **1994**, *91*, 9141–9145.
- (61) deSolms, S. J.; Deana, A. A.; Giuliani, E. A.; Graham, S. L.; Kohl, N. E.; Mosser, S. D.; Oliff, A. I.; Pompliano, D. L.; Rands, E.; Scholz, T. H.; Wiggins, J. M.; Gibbs, J. B.; Smith, R. L. Pseudopeptide Inhibitors of Protein Farnesyltransferase. *J. Med. Chem.* **1995**, *38*, 3967–3971.
- (62) Qian, Y.; Vogt, A.; Sebti, S. M.; Hamilton, A. D. Design and Synthesis of Non-Peptide Ras CAAAX Mimetics as Potent Farnesyltransferase Inhibitors. *J. Med. Chem.* **1996**, *39*, 217–223.
- (63) Leftheris, K.; Kline, T.; Vite, G. D.; Cho, Y. H.; Bhide, R. S.; Patel, D. V.; Patel, M. M.; Schmidt, R. J.; Weller, H. N.; Andahazy, M. L.; Carboni, J. M.; Gullo-Brown, J. L.; Lee, F. Y. F.; Ricca, C.; Rose, W. C.; Yan, N.; Barbacid, M.; Hunt, J. T.; Meyers, C. A.; Seizinger, B. R.; Zahler, R.; Manne, V. Development of Highly Potent Inhibitors of Ras Farnesyltransferase Possessing Cellular and in Vivo Activity. *J. Med. Chem.* **1996**, *39*, 224–236.
- (64) Hunt, J. T.; Lee, V. G.; Leftheris, K.; Seizinger, B.; Carboni, J.; Mabus, J.; Ricca, C.; Yan, N.; Manne, V. Potent, Cell Active, Non-Thiol Tetrapeptide Inhibitors of Farnesyltransferase. *J. Med. Chem.* **1996**, *39*, 353–359.
- (65) Williams, T. M.; Ciccarone, T. M.; MacTough, S. C.; Bock, R. L.; Conner, M. W.; Davide, J. P.; Hamilton, K.; Koblan, K. S.; Kohl, N. E.; Kral, A. M.; Mosser, S. D.; Omer, C. A.; Pompliano, D. L.; Rands, E.; Schaber, M. D.; Shah, D.; Wilson, F. R.; Gibbs, J. B.; Graham, S. L.; Hartman, G. D.; Oliff, A. I.; Smith, R. L. 2-Substituted Piperazines as Constrained Amino Acids. Application to the Synthesis of Potent, Non Carboxylic Acid Inhibitors of Farnesyltransferase. *J. Med. Chem.* **1996**, *39*, 1345–1348.
- (66) Daniele, M.; Shuler, K. R.; Poulter, C. J.; Eaton, S. R.; Sawyer, T. K.; Hodges, J. C.; Su, T.-Z.; Scholten, J. D.; Gowan, R. C.; Sebolt-Leopold, J. S.; Doherty, A. M. Structure-Activity Relationships of Cysteine-Lacking Pentapeptide Derivatives That Inhibit ras Farnesyltransferase. *J. Med. Chem.* **1997**, *40*, 192–200.
- (67) McNamara, D. J.; Dobrusin, E.; Leonard, D. M.; Shuler, K. R.; Kaltenbronn, James S.; Quin, J., III; Bur, S.; Thomas, C. E.; Doherty, A. M.; Scholten, J. D.; Zimmerman, K. K.; Gibbs, B. S.; Gowan, R. C.; Latash, M. P.; Leopold, W. R.; Przybranowski, S. A.; Sebolt-Leopold, J. S. C-Terminal Modifications of Histidyl-N-benzylglycinamides To Give Improved Inhibition of Ras Farnesyltransferase, Cellular Activity, and Anticancer Activity in Mice. *J. Med. Chem.* **1997**, *40*, 3319–3322.
- (68) Njoroge, F. G.; Vibulbhan, B.; Rane, D. F.; Bishop, W. R.; Petrin, J.; Patton, R.; Bryant, M. S.; Chen, K.-J.; Nomeir, A. A.; Lin, C.-C.; Liu, M.; King, I.; Chen, J.; Lee, S.; Yaremko, B.; Dell, J.; Lipari, P.; Malkowski, M.; Li, Z.; Catino, J.; Doll, R. J.; Girijavallabhan, V. M.; Ganguly, A. K. Structure-Activity Relationship of 3-Substituted N-(Pyridinylacetyl)-4-(8-chloro-5,6-dihydro-11H-benzol[5,6]cyclohepta[1,2-b]pyridine-11-ylidene)-piperidine Inhibitors of Farnesyl-Protein Transferase: Design and Synthesis of in Vivo Active Antitumor Compounds. *J. Med. Chem.* **1997**, *40*, 4290–4301.
- (69) Aoyama, T.; Satoh, T.; Yonemoto, M.; Shibata, J.; Nonoshita, K.; Arai, S.; Kawakami, K.; Iwasawa, Y.; Sano, H.; Tanaka, K.; Monden, Y.; Kodera, T.; Arakawa, H.; Suzuki-Takahashi, I.; Kamei, T.; Tomimoto, K. A New Class of Highly Potent Farnesyl Diphosphate-Competitive Inhibitors of Farnesyltransferase. *J. Med. Chem.* **1998**, *41*, 143–147.
- (70) Njoroge, F. G.; Vibulbhan, B.; Pinto, P.; Bishop, W. R.; Bryant, M. S.; Nomeir, A. A.; Lin, C.-C.; Liu, M.; Doll, R. J.; Girijavallabhan, V.; Ganguly, A. K. Potent, Selective, and Orally Bioavailable Tricyclic Pyridyl Acetamide N-Oxide Inhibitors of Farnesyl Protein Transferase with Enhanced in Vivo Antitumor Activity. *J. Med. Chem.* **1998**, *41*, 1561–1567.
- (71) deSolms, S. J.; Giuliani, E. A.; Graham, S. L.; Koblan, K. S.; Kohl, N. E.; Mosser, S. D.; Oliff, A. I.; Pompliano, D. L.; Rands, E.; Scholz, T. H.; Wiscourt, C. M.; Gibbs, J. B.; Smith, R. L. N-Arylalkyl Pseudopeptide Inhibitors of Farnesyltransferase. *J. Med. Chem.* **1998**, *41*, 2651–2656.
- (72) Augeri, D. J.; O'Connor, S. J.; Janowick, D.; Szczepankiewicz, B.; Sullivan, G.; Larsen, J.; Kalvin, D.; Cohen, J.; Devine, E.; Zhang, H.; Cherian, S.; Saeed, B.; Ng, S.-C.; Rosenberg, S. Potent and Selective Non-Cysteine-Containing Inhibitors of Protein Farnesyltransferase. *J. Med. Chem.* **1998**, *41*, 4288–4300.
- (73) Lingham, R. B.; Silverman, K. C.; Jayasuriya, H.; Kim, B. M.; Amo, S. E.; Wilson, F. R.; Rew, D. J.; Schaber, M. D.; Bergstrom, J. D.; Koblan, K. S.; Graham, S. L.; Kohl, N. E.; Gibbs, J. B.; Singh, S. B. Clavarinic Acid and Steroid Analogues as Ras- and FPP-Directed Inhibitors of Human Farnesyl-Protein Transferase. *J. Med. Chem.* **1998**, *41*, 4492–4501.
- (74) Njoroge, F. G.; Taveras, A. G.; Kelly, J.; Remiszewski, S.; Mallams, A. K.; Wolin, R.; Afonso, A.; Cooper, A. B.; Rane, D. F.; Liu, Y.-T.; Wong, J.; Vibulbhan, B.; Pinto, P.; Deskus, J.; Alvarez, C. S.; del Rosario, J.; Connolly, M.; Wang, J.; Desai, J.; Rossman, R. R.; Bishop, W. R.; Patton, R.; Wang, L.; Kirschmeier, P.; Bryant, M. S.; Nomeir, A. A.; Lin, C.-C.; Liu, M.; McPhail, A. T.; Doll, R. J.; Girijavallabhan, V. M.; Ganguly, A. K. (+)-4-[2-[4-(8-Chloro-3,10-dibromo-6-11-dihydro-5H-benzol[5,6]cyclohepta[1,2-b]pyridin-11(R)-yl]-1-piperidinyl]-1-oxo-ethyl]-1-piperidinecarboxamide (SCH-66336): A Very Potent Farnesyl Protein Transferase Inhibitor as a Novel Antitumor Agent. *J. Med. Chem.* **1998**, *41*, 4890–4902.
- (75) Roskoski, R., Jr.; Ritchie, P. Role of the Carboxyterminal Residue in Peptide Binding to Protein Farnesyltransferase and Protein Geranylgeranyltransferase. *Arch. Biochem. Biophys.* **1998**, *356*, 167–176.
- (76) Barber, A. M.; Hardcastle, I. R.; Rowlands, M. G.; Nutley, B. P.; Marriott, J. H.; Jarman, M. Solid-phase synthesis of novel inhibitors of farnesyl transferase. *Bioorg. Med. Chem. Lett.* **1999**, *9*, 623–626.
- (77) Augeri, D. J.; Janowick, D.; Kalvin, D.; Sullivan, G.; Larsen, J.; Dickman, D.; Ding, H.; Cohen, J.; Lee, J.; Warner, R.; Kovar, P.; Cherian, S.; Saeed, B.; Zhang, H.; Tahir, S.; Ng, S.-C.; Sham, H.; Rosenberg, S. H. Potent and Orally Bioavailable Noncysteine-Containing Inhibitors of Protein Farnesyltransferase. *Bioorg. Med. Chem. Lett.* **1999**, *9*, 623–626.
- (78) Vasudevan, A.; Qian, W.; Vogt, A.; Blaskovich, M. A.; Ohkanda, J.; Sebti, S. M.; Hamilton, A. D. Potent, Highly Selective, and Non-Thiol Inhibitors of Protein Geranylgeranyltransferase-I. *J. Med. Chem.* **1999**, *42*, 1333–1340.
- (79) Taveras, A. G.; Deskus, J.; Chao, J.; Vaccaro, C. J.; Njoroge, F. G.; Vibulbhan, B.; Pinto, P.; Remiszewski, S.; del Rosario, J.; Doll, R. J.; Alvarez, C.; Lalwani, T.; Mallams, A. K.; Rossman, R. R.; Afonso, A.; Girijavallabhan, V. M.; Ganguly, A. K.; Pramanik, B.; Heimark, L.; Bishop, W. R.; Wang, L.; Kirschmeier, P.; James, L.; Carr, D.; Patton, R.; Bryant, M. S.; Nomeir, A. A.; Liu, M. Identification of Pharmacokinetically Stable 3,10-Dibromo-8-chlorobenzocycloheptapyridine Farnesyl Protein Transferase Inhibitors with Potent Enzyme and Cellular Activities. *J. Med. Chem.* **1999**, *42*, 2651–2661.
- (80) Anthony, N. J.; Gomez, R. P.; Schaber, M. D.; Mosser, S. D.; Hamilton, K. A.; O'Neil, T. J.; Koblan, K. S.; Graham, S. L.; Hartman, G. D.; Shah, D.; Rands, E.; Kohl, N. E.; Gibbs, J. B.; Oliff, A. I. Design and in Vivo Analysis of Potent Non-Thiol Inhibitors of Farnesyl Protein Transferase. *J. Med. Chem.* **1999**, *42*, 3356–3368.
- (81) O'Connor, S. J.; Barr, K. J.; Wang, L.; Sorensen, B. K.; Tasker, A. S.; Sham, H.; Ng, S.-C.; Cohen, J.; Devine, E.; Cherian, S.; Saeed, B.; Zhang, H.; Lee, J. Y.; Warner, R.; Tahir, S.; Kovar, P.; Ewing, P.; Alder, J.; Mitten, M.; Leal, J.; Marsh, K.; Bauch, J.; Hoffman, D. J.; Sebti, S. M.; Rosenberg, S. H. Second Generation Peptidomimetic Inhibitors of Protein Farnesyltransferase Demonstrating Improved Cellular Potency and Significant in Vivo Efficacy. *J. Med. Chem.* **1999**, *42*, 3701–3710.
- (82) Williams, T. M.; Bergman, J. M.; Brashear, K.; Breslin, M. J.; Dinsmore, C. J.; Hutchinson, J. H.; MacTough, S. C.; Stump, C. A.; Wei, D. D.; Zartman, C. B.; Ghusky, M. J.; Culbertson, J. C.; Buser-Doepner, C.; Davide, J.; Greenberg, I. B.; Hamilton, K. A.; Koblan, K. S.; Kohl, N. E.; Liu, D.; Lobell, R. B.; Mosser, S. D.; O'Neill, T. J.; Rands, E.; Schaber, M. D.; Wilson, F.; Senderak, E.; Motzel, S. L.; Gibbs, J. B.; Graham, S. L.; Heimbrook, D. C.; Hartman, G. D.; Oliff, A. I.; Huff, J. R. N-Arylpiperazinone Inhibitors of Farnesyltransferase: Discovery and Biological Activity. *J. Med. Chem.* **1999**, *42*, 3779–3784.



- (83) Gibbs, B. S.; Zahn, T. J.; Mu, Y.; Sebolt-Leopold, J. S.; Gibbs, R. A. Novel Farnesol and Geranylgeraniol Analogues: A Potential New Class of Anticancer Agents Directed against Protein Prenylation. *J. Med. Chem.* **1999**, *42*, 3800–3808.
- (84) Henry, K. J., Jr.; Wasicak, J.; Tasker, A. S.; Cohen, J.; Ewing, P.; Mitten, M.; Larsen, J. J.; Kalvin, D. M.; Swenson, R.; Ng, S.-C.; Saeed, B.; Cherian, S.; Sham, H.; Rosenberg, S. H. Discovery of a Series of Cyclohexylethylamine-Containing Protein Farnesyltransferase Inhibitors Exhibiting Potent Cellular Activity. *J. Med. Chem.* **1999**, *42*, 4844–4852.
- (85) Lawrence, D. S.; Zilfou, J. T.; Smith, C. D. Structure–Activity Studies of Cerulenin Analogues as Protein Palmitoylation Inhibitors. *J. Med. Chem.* **1999**, *42*, 4932–4941.
- (86) Ding, C. Z.; Batorsky, R.; Bhide, R.; Chao, H. J.; Cho, Y.; Chong, S.; Gullo-Brown, J. i.; Guo, P.; Kim, S. H.; Lee, F.; Leftheris, K.; Miller, A.; Mitt, T.; Patel, M.; Penhallow, B. A.; Ricca, C.; Rose, W. C.; Schmidt, R.; Slusarchyk, W. A.; Vite, G.; Yan, N.; Manne, V.; Hunt, J. T. Discovery and Structure–Activity Relationships of Imidazole-Containing Tetrahydrobenzodiazepine Inhibitors of Farnesyltransferase. *J. Med. Chem.* **1999**, *42*, 5241–5253.
- (87) O'Connor, C. E.; Ackermann, K.; Rowell, C. A.; Garcia, A. M.; Lewis, M. D.; Schwartz, C. E. Synthesis and Evaluation of Hydroxyproline-Derived Isoprenyltransferase Inhibitors. *Bioorg. Med. Chem. Lett.* **1999**, *9*, 2095–2100.
- (88) Tamanoi, F.; Gau, C.-L.; Jiang, C.; Edamatsu, H.; Kato-Stankiewicz, J. Protein farnesylation in mammalian cells: Effects of farnesyltransferase inhibitors on cancer cells. *Cell. Mol. Life Sci.* **2001**, *58*, 1636–1649.
- (89) Sakowski, J.; Sattler, I.; Schlitzer, M. Non-Thiol Farnesyltransferase Inhibitors: *N*-(4-Acylamino-3-benzoylphenyl)-4-nitrocinnamic Acid Amides. *Bioorg. Med. Chem.* **2002**, *10*, 233–239.
- (90) Chen, A. P.-C.; Chen, Y.-H.; Liu, H.-P.; Li, Y.-C.; Chen, C.-T.; Liang, P.-H. Synthesis and Application of a Fluorescent Substrate Analogue To Study Ligand Interactions for Undecaprenyl Pyrophosphate Synthase. *J. Am. Chem. Soc.* **2004**, *124*, 15217–15244.
- (91) Nara, S.; Tanaka, R.; Eishima, J.; Hara, M.; Otaki, S.; Foglesong, R. J.; Hughes, P. F.; Turkington, S.; Kanda, Y. Discovery and Structure–Activity Relationships of Novel Piperidine Inhibitors of Farnesyltransferase. *J. Med. Chem.* **2003**, *46*, 2467–2473.
- (92) Nara, S.; Tanaka, R.; Yoda, N.; Eishima, J.; Hara, M.; Soga, S.; Akinaga, S.; Ohashi, R.; Kuwabara, T.; Foglesong, R. J.; Hughes, P. F.; Turkington, S.; Kanda, Y. Structure–Activity Relationships of Novel Piperidine Derivatives as Ras Farnesyltransferase Inhibitors. Presented at the 5th AFMC International Medicinal Chemistry Symposium, Kyoto, Japan, October 14–17, 2003; Poster.
- (93) Tong, Y.; Lin, N.-H.; Wang, L.; Hasvold, L.; Wang, W.; Leonard, N.; Li, T.; Li, Q.; Cohen, J.; Gu, W.-Z.; Zhang, H.; Stoll, V.; Bauch, J.; Marsh, K.; Rosenberg, S. H.; Sham, H. L. *Bioorg. Med. Chem. Lett.* **2003**, *13*, 1571–1574.
- (94) Burden, F. R. Using Artificial Neural Networks To Predict Biological Activity from Simple Molecular Structure Considerations. *Quant. Struct.–Act. Relat.* **1996**, *15*, 7–11.
- (95) Burden, F. R. Molecular Identification Number for Substructure Searches. *J. Chem. Inf. Comput. Sci.* **1989**, *29*, 225–227.
- (96) Burden, F.; Winkler, D. A.; Polley, M. Manuscript in preparation.
- (97) Gasteiger, J.; Marsili, M. Iterative Partial Equalization of Orbital Electronegativity—A Rapid Access to Atomic Charges. *Tetrahedron* **1980**, *36*, 3219–3288.
- (98) Estrada, E.; Pena, A.; Garcia-Domenech, R. Designing sedative/hypnotic compounds from a novel substructural graph-theoretical approach. *J. Comput.-Aided Mol. Des.* **1998**, *12*, 583–595.

JM049621J